LS-138
Mansoo Choi
June 15, 1989
(w/rev. 10/24/89)

A Note on Thermal Analysis for an Inclined Plate Crotch Absorber

1 INTRODUCTION

Crotch absorbers are used to absorb unwanted synchrotron radiation to prevent most of the photons from striking the wall of a vacuum chamber. Since synchrotron radiation generated by bending the positron beam is very powerful, concentrated and penetrating, the absorber produces high internal heat generation. Depending on the materials used, this energy generation may be restricted near the surface of the absorber or distributed throughout the absorber with exponential decay in the direction of the penetration. The cooling of an absorber is important to prevent melting the material and to retain ultra high vacuum, since photon energy deposition on the metal surface causes the desorption of gases.

This note is mainly about thermal aspects of highly concentrated photon beam penetration through the inclined metal plates. Inclined crotch absorbers were considered to reduce the high wall heat flux at LBL, SSRL and ESRF. Note that when the plate is inclined, the area is increased by a factor of $1/\sin\theta$, where θ is the angle between the plate and the incident photon beam (e.g., the case of $\theta = \pi/2$ should have the highest heat flux). It is also pointed out that inclination of the absorber enhances photon reflection and photo-electron production, both deterimental to UHV, and it would be desirable to optimize inclination considering both the heat flux and the gas desorption.

This note describes an analytical solution of the heat transfer with application to designing a crotch absorber. The effects of angles and thicknesses of the plate and different materials on temperature distributions of the absorber are examined.

2 ANALYSIS

For high Z materials, most of the photon energy is absorbed very near the surface because the absorption coefficient generally becomes larger as Z increases. Therefore, it is reasonable to assume the incident photon energy deposits on the surface for high Z material (e.g., copper with Z=29). However, for low Z materials such as beryllium (Z=4), photons

penetrate with relative ease; correspondingly, photon energy deposition will be distributed through a significant depth of the plate, and the assumption of surface deposition is no longer valid. In this note, the general case of a penetrating photon beam heating through an inclined plate will be discussed (the present solution includes cases of the surface deposition and the vertical plate).

Consider an inclined plate with angle θ with respect to the incident photon beam (see Figure 1). For a homogeneous material, the heat conduction equation (including heat generation) may be written for constant thermal conductivity:

$$\nabla^2 T = \frac{-f(x,y)}{k} \tag{1}$$

Considering that the photon beam passes with a tilted angle θ with respect to the coordinate x, the heat generation $f(x,y)$ due to the absorption was obtained :

$$f(x,y) = \int_0^\infty \alpha_\lambda I_o(-x cos\theta + (y - b/2) sin\theta, \lambda) \cdot exp(-\alpha_\lambda \frac{x}{sin\theta}) d\lambda \tag{2}$$

where I_o, α_λ and λ are the incident synchrotron radiation, the absorption coefficient of a metal and the wavelength of the photons, respectively. Note that the value in the parenthesis of I_o designates the vertical length from the center of the photon beam, which corresponds to the location (x,y). Boundary conditions and dimensions are given in Figure 1.

Using Fourier's method, a series form of the two dimensional solution may be written

$$T - T_\infty = \sum_{m=1}^{\infty} \sum_{n=1}^{\infty} A_{mn} cos\sqrt{\lambda_m}\, x cos\frac{n\pi y}{b} + \sum_{m=1}^{\infty} B_m cos\sqrt{\lambda_m}\, x \tag{3}$$

and coefficients A_{mn} and B_m are given as follows;

$$A_{mn} = \frac{\int_0^a \int_0^b f(x,y) cos\sqrt{\lambda_m}\, x cos\frac{n\pi y}{b} dx dy}{-(\lambda_m + (\frac{n\pi}{b})^2)(\frac{a}{2} + \frac{sin2\sqrt{\lambda_m} a}{4\sqrt{\lambda_m}})\frac{b}{2}} \tag{4}$$

$$B_m = \frac{\int_0^a \int_0^b f(x,y) cos\sqrt{\lambda_m} x dx dy}{-\lambda_m (\frac{a}{2} + \frac{sin2\sqrt{\lambda_m} a}{4\sqrt{\lambda_m}}) b} \tag{5}$$

where $\sqrt{\lambda_m}$, a and b are the eigenvalue, the thickness of the plate and the width of the plate, respectively. The values of $\sqrt{\lambda_m}$ can be calculated from

$$-\sqrt{\lambda_m}tan\sqrt{\lambda_m}a = h$$

where h is the heat transfer coefficient.

The absorption coefficient, α_λ, is dependent on photon energy. In this note, it is assumed that this has the constant value corresponding to the critical energy of the synchrotron radiation from a bending magnet. It is noted that lengthy numerical integrations associated with equations (2), (4) and (5) would be required to include the variation of the absorption coefficient, which is a function of spectral incident synchrotron radiation, and a closed form of the coefficients could not be sought. The case of variable absorption coefficients will be discussed in a subsequent note where a numerical analysis is presented.

The synchrotron radiation power density integrated with respect to wavelength as a function of the vertical coordinate y' is given:

$$P_D = \int_0^\infty I_o(y',\lambda)d\lambda = \frac{12.4E^4BI}{l^2}\cdot 0.4375exp(-(\frac{\gamma y'}{0.608l})^2/2)\ [kw/m^2] \tag{6}$$

where E, I, B, l and γ are the positron energy in GeV, the positron beam current in mA, the magnetic field of bending magnet in T, the tangential length from the source to the plate in m and $\gamma = \frac{E}{m_o c^2} = 1957E$, respectively. Substitution of the above equation into equation (2) yields:

$$f(x,y) = C\cdot\alpha_\lambda exp(-\alpha_\lambda\frac{x}{sin\theta})\cdot exp(-(\frac{\gamma(-xcos\theta+(y-b/2)sin\theta)}{0.608l})^2/2) \tag{7}$$

where C is equal to $\frac{5425E^4BI}{l^2}$. The integration and substitution of equation (7) into equations (4) and (5) were carried out and A_{mn} and B_m are obtained in closed forms:

$$A_{mn} = \frac{C\sqrt{\pi}exp(-\frac{p^2}{4q^2})\alpha_\lambda}{-(\lambda_m+(\frac{n\pi}{b})^2)(\frac{a}{2}+\frac{sin2\sqrt{\lambda_m}a}{4\sqrt{\lambda_m}})qbsin\theta/2}\cdot(I_{B1}+I_{B2}) \tag{8}$$

$$B_m = \frac{C\sqrt{\pi}\alpha_\lambda}{-\lambda_m(\frac{a}{2}+\frac{sin2\sqrt{\lambda_m}a}{4\sqrt{\lambda_m}})qbsin\theta}\cdot\frac{exp(-\frac{\alpha_\lambda a}{sin\theta})(-\frac{\alpha_\lambda}{sin\theta}cos\sqrt{\lambda_m}a+\sqrt{\lambda_m}sin\sqrt{\lambda_m}a)+\frac{\alpha_\lambda}{sin\theta}}{(\frac{\alpha_\lambda}{sin\theta})^2+\lambda_m} \tag{9}$$

where

$$I_{B1}\ or\ I_{B2} = \frac{0.5exp(\frac{\alpha_\lambda a_{1\,or\,2}}{sin\theta})}{(\frac{\alpha_\lambda}{sin\theta})^2 + (\sqrt{\lambda_m} \mp pcos\theta)^2} \cdot \left(exp(-\frac{\alpha_\lambda(a + a_{1\,or\,2})}{sin\theta}) \left(-\frac{\alpha_\lambda}{sin\theta} \cdot \right.\right.$$

$$\left. \cdot cos(\sqrt{\lambda_m} \mp pcos\theta)(a + a_{1\,or\,2}) + (\sqrt{\lambda_m} \mp pcos\theta) sin(\sqrt{\lambda_m} \mp pcos\theta)(a + a_{1\,or\,2}) \right) - exp(-\frac{\alpha_\lambda a_{1\,or\,2}}{sin\theta}) \cdot$$

$$\left. \cdot \left(-\frac{\alpha_\lambda}{sin\theta} cos(\sqrt{\lambda_m} \mp pcos\theta) a_{1\,or\,2} + (\sqrt{\lambda_m} \mp pcos\theta) sin(\sqrt{\lambda_m} \mp pcos\theta) a_{1\,or\,2} \right) \right),$$

$$a_{1\,or\,2} = \mp \frac{bpsin\theta}{2(\sqrt{\lambda_m} \mp pcos\theta)},$$

$$p = \frac{n\pi}{bsin\theta},$$

$$q = \frac{\gamma}{0.608l\sqrt{2}}$$

The remaining task to be performed to obtain the temperature field is the summation of infinite series. The maximum numbers of m and n were tested to yield results independent of upper limits of m and n. The appropriate values of upper limits of m and n are found to be several hundreds and thousands, respectively. To accelerate the convergence of the above series, Shanks' transformation was used and shown to accelerate two or three times faster than direct summations and produce results within one percent disagreement with direct summations. The following Shanks transformation was utilized:

$$S(H_n) = \frac{H_{n+1}H_{n+1} - H_n^2}{H_{n+1} + H_{n-1} - 2H_n}$$

$$H_n = \sum_{k=1}^{n} C_k$$

3 RESULTS AND DISCUSSIONS

Table 1 shows the design parameters for various bending magnet sources that are currently proposed or in construction. In Table 1, Q_{max}'s were calculated using equation (6), except the one that ESRF reported. It is shown that the APS absorber has the highest heat

flux (approximately 40% higher than RIKEN and 16% higher than ESRF) of the current proposed machines.

Figure 2-1 shows the effect of different thicknesses of the plate on the maximum surface temperatures for a vertical Cu plate. As the thickness increases, the water cooled surface temperature decreases monotonically while the temperature of the vacuum surface, which faces on ultra high vacuum, decreases and then increases. As the plate becomes thicker, the water cooled surface temperature becomes more uniform due to the diffusion of the heat, and water cooling occurs over the broader region of the water contact surface so that the maximum water surface temperature becomes less (see Figure 2-2). It is also noted that while small thickness allows the water cooled surface to get closer to the vacuum surface, it also causes the maximum temperature of the water cooled surface to become higher than with thicker plates. It is shown in Figure 2-1 that the rapid decrease of the water cooled surface temperature when the thickness a increases from 5 mm to 1 cm causes the vacuum surface to have a lower temperature, despite the fact it is getting farther from the water cooled surface. Further increase of the thickness increases the vacuum surface temperature due to larger distance from the water cooled surface. Vacuum surface temperatures exceed 900 K for all cases with the vertical Cu plate, and the water cooled surface temperatures may fall below 423 K (saturation temperature at p = 0.48 MPa) for the plates with larger thickness than 2 cm.

Table 2 shows the effect of inclination angles on surface temperatures. As the angle between the plate and the incident photon beam becomes smaller (more inclined), the maximum surface temperatures decrease as a result of reduced peak power density. However, the maximum water channel temperatures remain almost same. This is because the vertically inclined plate absorbs the same total energy regardless of inclined angles. The reduced peak power density does not affect the water channel temperature since the localized heating on the surface is sufficiently diffused through the 2 cm thick copper plate. It is noted that even at 10 degree (vertically rotated angle ; refer to Fig. 1) which would be the maximum inclination due to the space restriction, the surface temperature reaches beyond $500°C$. Alternatives to reduce the maximum surface and water channel temperatures would be 1) horizontally rotated absorber 2) the use of beryllium inserted two layer plate. When the plate is rotated horizontally, the total energy deposited per unit length as well as the peak power density become reduced by factor of $sin\theta_1$ (θ_1 is the angle rotated horizontally) while for the vertically rotated case, the total energy deposited

per unit length remains the same. On the other hand, the horizontally rotated case would need more cooling channels due to the increased photon reception areas in the spanwise direction than the vertically rotated one. The present solution could be extended to the horizontally rotated case for which

$$f(x,y) = sin\theta_1 \int_0^\infty \alpha_\lambda I_o((y-b/2),\lambda) \cdot exp(-\alpha_\lambda \frac{x}{sin\theta_1}) d\lambda$$

Therefore, equations (8) and (9) would be modified replacing $C = \frac{5425E^4BIsin\theta_1}{l^2}$, $\theta = 90$ and $\frac{\alpha_\lambda}{sin\theta}$ by $\frac{\alpha_\lambda}{sin\theta_1}$. Especially for high Z material such as copper for which the surface deposition can be assumed (i.e. α_λ becomes large), ΔT_h for horizonally rotated angle θ_1 would be approximately equal to $sin\theta_1 \cdot \Delta T_v(\theta = 90)$ where ΔT_h and ΔT_v are the temperature increases for horizontally and vertically rotated cases, respectively. For example, for $\theta_1 = 30°$ of copper, $T_{max} \approx 362°C$ and $T_{water} \approx 97°C$ (refer to the vertically inclined case of $\theta = 30°$ in Table 2). Further study of horizontally rotated absorbers is being carried out and the case of Be-Cu two layer inclined absorber is also under investigation.

The reason the temperatures for Be plates are lower than those for Cu plates despite their having lower conductivity than copper is that the incident radiation not only deposits throughout the plate, but also a portion of incident radiation penetrates through the inclined Be plate (for example, approximately 40 % of the total photon energy penetrates through a 2 cm thick vertical Be plate in this analysis while virtually all energy is absorbed for a copper plate). As Be plate is further inclined vertically, the photon penetration path becomes longer, correspondingly, more photons are absorbed and the surface temperature becomes higher as can be seen in table 2.

Figures 3-1 and 3-2 show isotherm lines for inclined Cu and Be plates with 30 degree tilt angle. It is shown that the Cu plate has almost symmetric temperature fields with respect to the center line of the plate through y=0 due to a large absorption coefficient which results in energy deposition being very near the surface. For a Be plate, Fig.3-2 shows the penetrating power of the photon beam, which results in asymmetric temperature fields.

In summary, an analytical solution was obtained for inclined plate crotch absorbers, and the effects of different materials, thicknesses and angles were examined. It is shown that vertically inclined Cu plate crotch absorbers do not appear to effectively manage the high

energy generation and as possible alternatives, horizontally rotated absorber and Be-Cu two layer absorber are being under investigation.

Table 1 Design parameters of various bending magnet sources

	APS	RIKEN	ESRF
E (GeV)	7	8	6
B (T)	0.6	0.6	0.8
I (mA)	300	100	200
l (m)	2.25 *	2	?
Qmax (W/mm^2)	463	333	400

*This value corresponds to the distance from the middle of BM to the crotch. The value of l (m) varies from 1.75 m to 3.61 m depending on the spanwise location of photon deposition.

Table 2 Maximum temperatures of the surfaces of the inclined Cu and Be plates

	copper		*beryllium*	
θ , o,	T_{max} , C	T_{water}	T_{max}	T_{water}
90	694	164	267	158
70	691	164	271	158
50	678	164	291	155
30	647	164	318	154
10	555	164	363	155

(k=386 W/m K for Cu and k= 185 W/m K for Be, h=12000 W/m^2 K, 2 cm thickness plate)

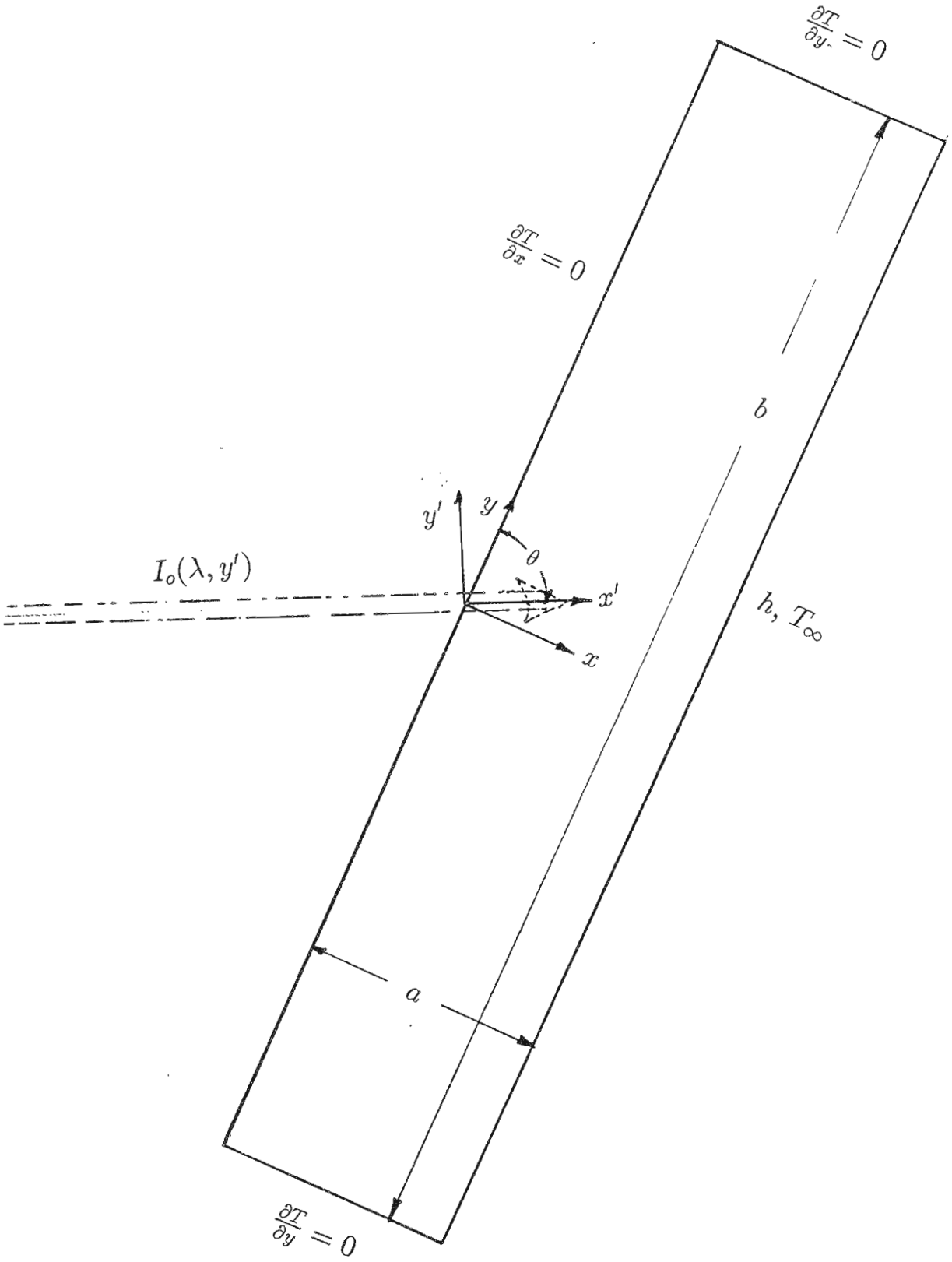

Fig. 1 Geometry and boundary conditions of the inclined plate absorber

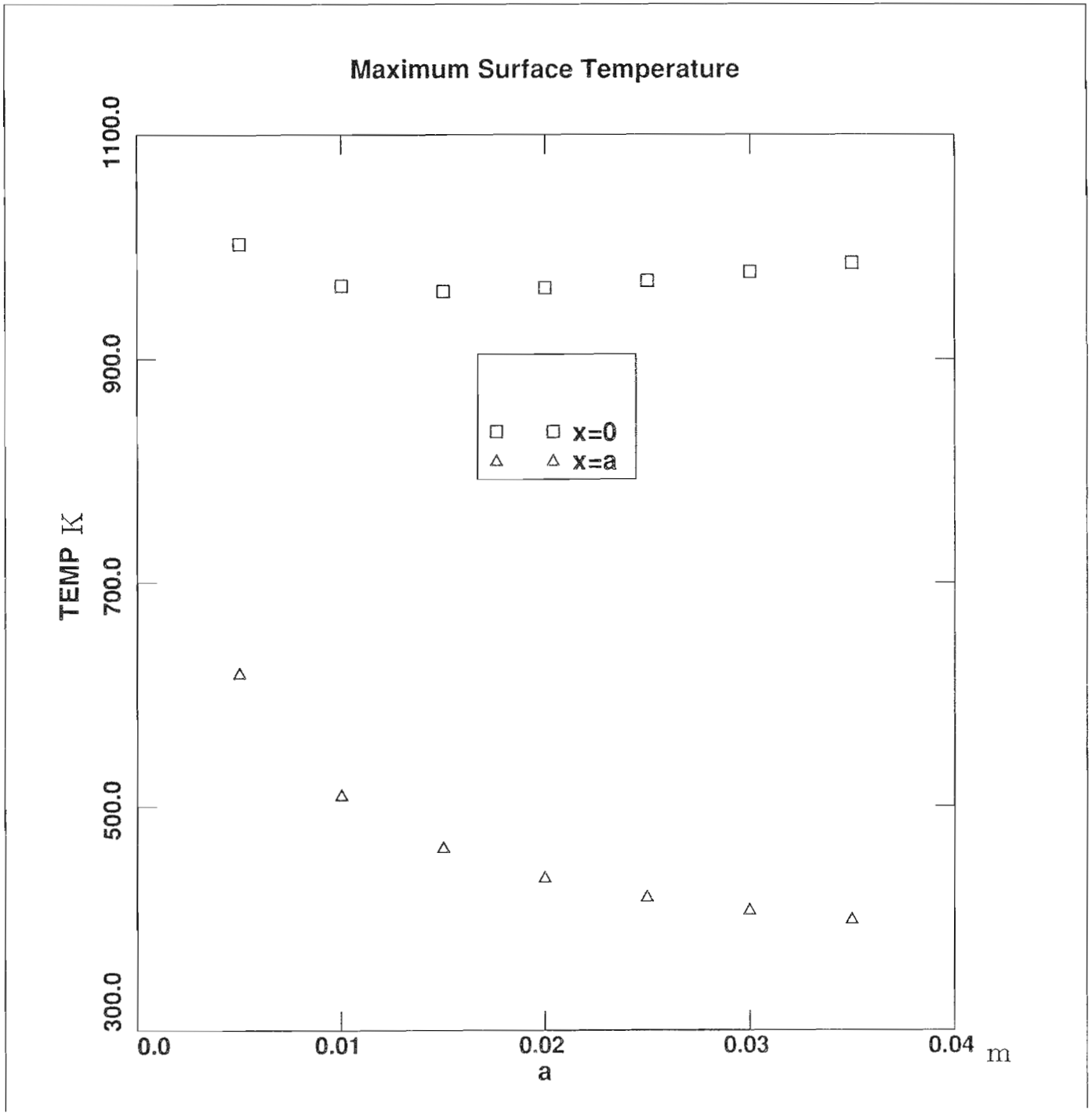

Fig. 2-1 Maximum temperatures of the surfaces of a vertical Cu plate

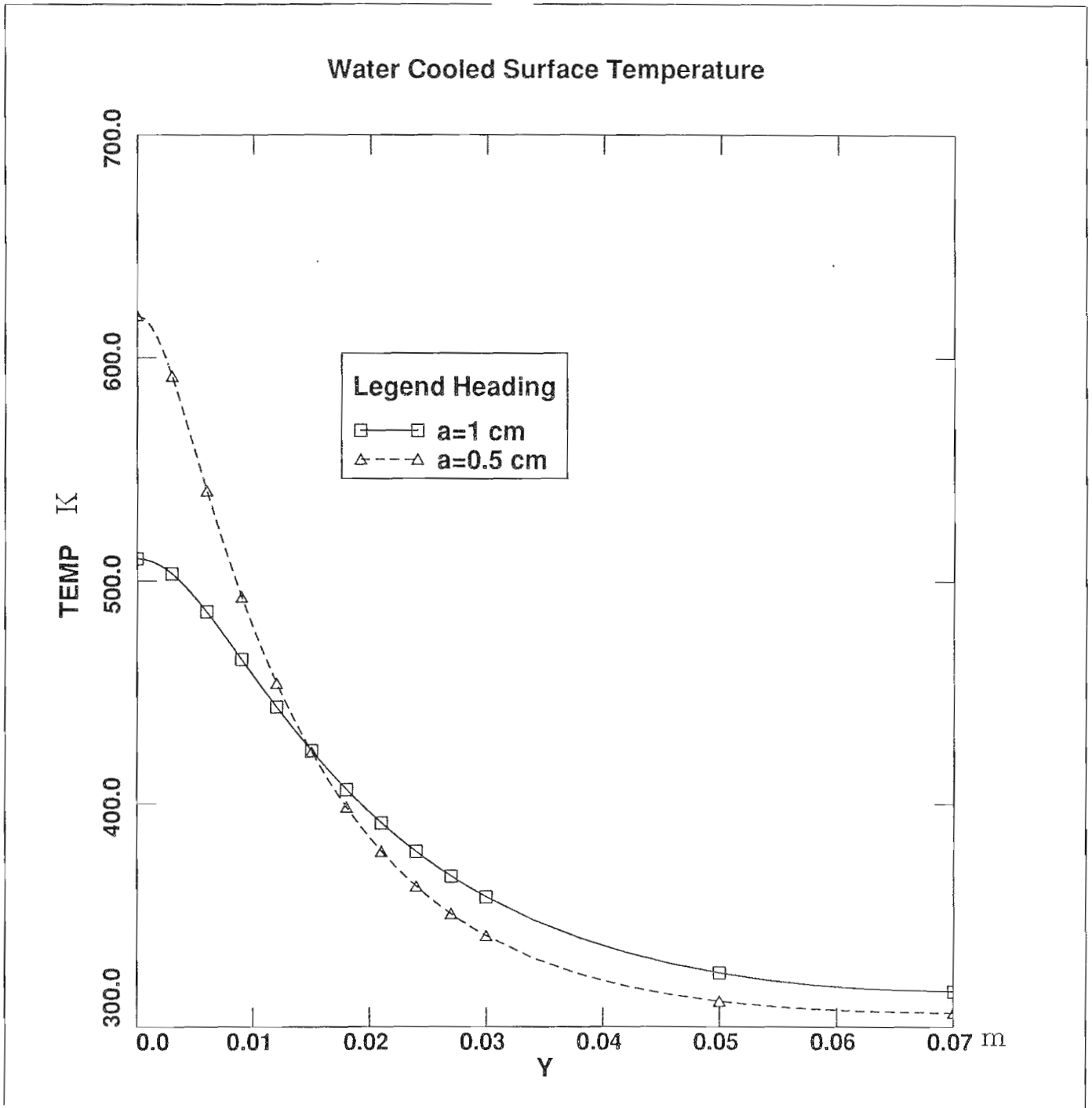

Fig. 2-2 Temperature distribution of the water cooled surface

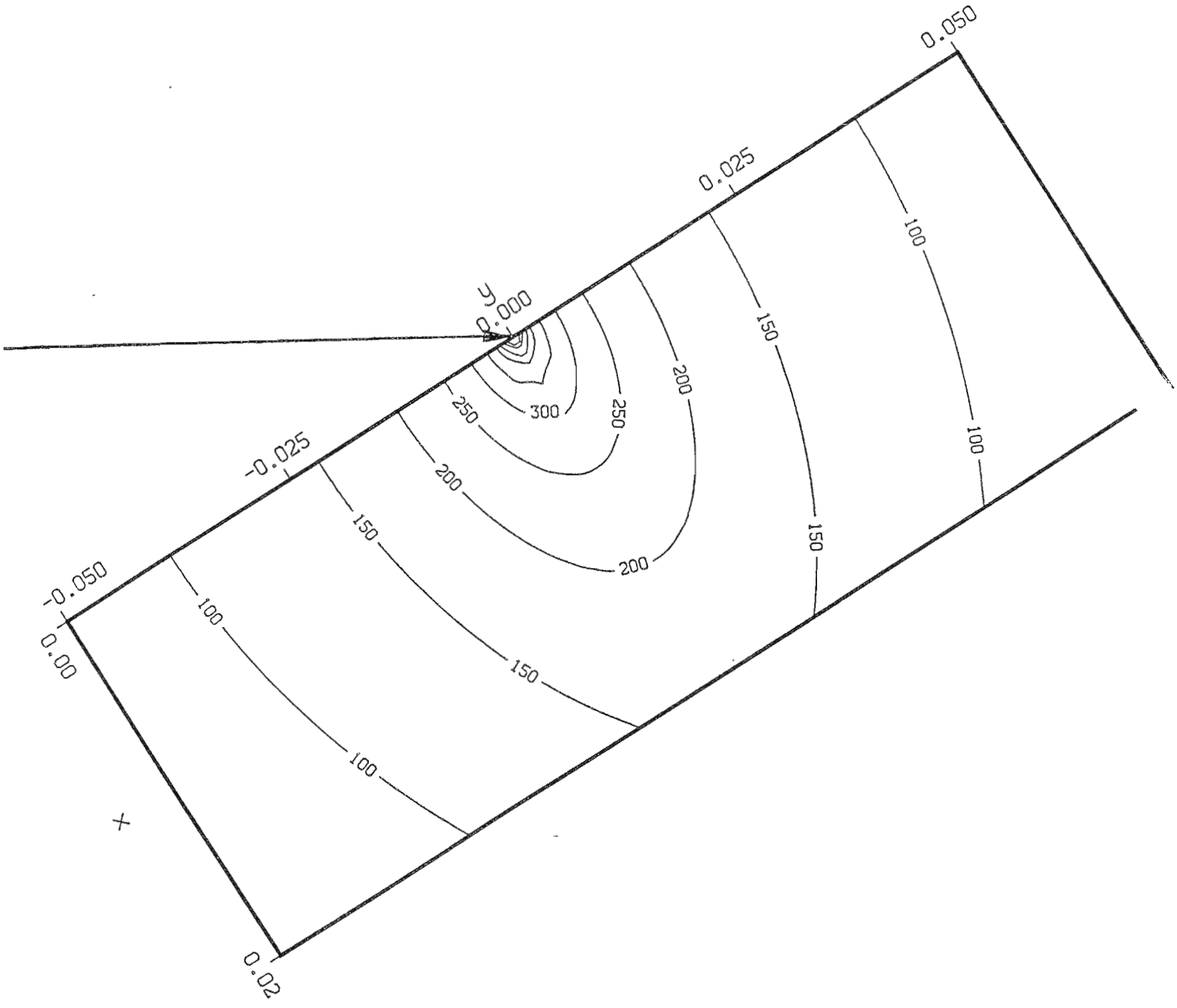

Fig. 3-1 Isotherm lines of an inclined Cu plate with 30 degree tilt angle

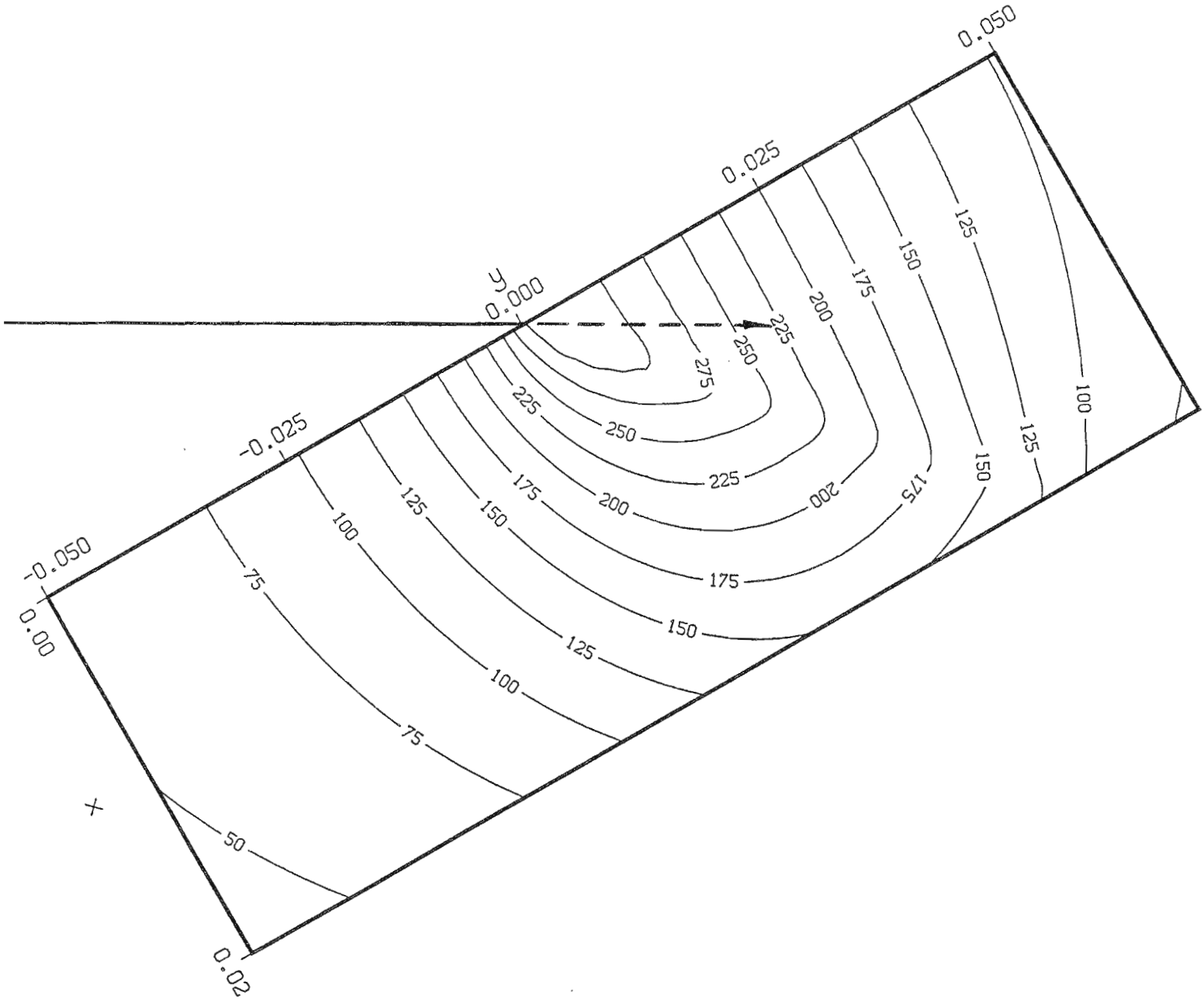

Fig. 3-2 Isotherm lines of an inclined Be plate with 30 degree tilt angle